

We thank D. Cassidy for sampling of the RISP cores, L. Burckle for assistance with diatom taxonomy, K. Austin for sample preparation and G. H. Denton and T. J. Hughes for discussions and for reading drafts of the manuscript. P. Whiting drafted the figure and C. McGowen typed the manuscript. This work was supported by NSF grants DPP-7721083 A01 and DPP-7920112.

Received 7 October 1980; accepted 30 June 1981.

1. Kellogg, T. B., Osterman, L. E. & Stuiver, M. *J. Foram. Res.* **9**, 322-335 (1979).
2. Kellogg, T. B. & Truesdale, R. S. *Mar. Micropalaeont.* **4**, 137-158 (1979).
3. Kellogg, T. B., Truesdale, R. S. & Osterman, L. E. *Geology* **7**, 249-253 (1979).
4. Opdyke, N. D. *Rev. Geophys. Space Phys.* **10**, 213-249 (1972).
5. McCollum, D. W. *Init. Rep. DSDP* **28**, 515-571 (1975).
6. Brady, H. T. & Martin, H. *Science* **203**, 437-438 (1979).
7. Webb, P. N., Ronan, T. E. Jr, Lipps, J. H. & DeLaca, T. E. *Science* **203**, 435-437 (1979).
8. Webb, P. N. *RISP tech. Rep. 78-1* (University of Nebraska, 1978); *RISP tech. Rep. 79-1* (University of Nebraska, 1979).
9. Brady, H. T. *Antarct. J. U.S.* **13**, 123-124 (1978); **14**, 130 (1979).
10. Truesdale, R. S. & Kellogg, T. B. *Mar. Micropalaeont.* **4**, 13-31 (1979).
11. Ling, H. Y. & White, R. J. *Antarct. J. U.S.* **14**, 126-127 (1979).
12. Lipps, J. H., Ronan, T. E. Jr & DeLaca, T. E. *Science* **203**, 447-449 (1979).
13. Schrader, H. J. *Nova Hedwigia* **45**, Suppl. 403-409 (1974).
14. Schrader, H. J. *Int. Rep. DSDP* **18**, 673-797 (1973); **35**, 605-671 (1976).
15. Fenner, J. *Init. Rep. DSDP* **39**, 491-623 (1977).
16. Webb, P. N. *Mem. natn. Inst. Polar Res.* **13**, 148-149 (1979).
17. Jacobs, S. S., Gordon, A. L. & Ardai, J. L. Jr *Science* **203**, 439-443 (1979).
18. Stuiver, M., Denton, G. H., Hughes, T. J. & Fastook, J. L. in *The Last Great Ice Sheets* (eds Denton, G. H. & Hughes, T. J.) 319-436 (Wiley, New York, 1981).
19. Kellogg, D. E., Stuiver, M., Kellogg, T. B. & Denton, G. H. *Palaeogeogr. Palaeoclimatol. Palaeoecol.* **30**, 157-189 (1980).
20. Boulton, G. S. J. *Glaciol.* **24**, 244 (1979).
21. Webb, P. N. & Brady, H. T. *EOS* **59**, 309 (1978).
22. Webb, P. N. *Mem. natn. Inst. Polar Res.* **13**, 206-212 (1979).

## A computer algorithm for reconstructing a scene from two projections

H. C. Longuet-Higgins

Laboratory of Experimental Psychology, University of Sussex, Brighton BN1 9QG, UK

A simple algorithm for computing the three-dimensional structure of a scene from a correlated pair of perspective projections is described here, when the spatial relationship between the two projections is unknown. This problem is relevant not only to photographic surveying<sup>1</sup> but also to binocular vision<sup>2</sup>, where the non-visual information available to the observer about the orientation and focal length of each eye is much less accurate than the optical information supplied by the retinal images themselves. The problem also arises in monocular perception of motion<sup>3</sup>, where the two projections represent views which are separated in time as well as space. As Marr and Poggio<sup>4</sup> have noted, the fusing of two images to produce a three-dimensional percept involves two distinct processes: the establishment of a 1:1 correspondence between image points in the two views—the 'correspondence problem'—and the use of the associated disparities for determining the distances of visible elements in the scene. I shall assume that the correspondence problem has been solved; the problem of reconstructing the scene then reduces to that of finding the relative orientation of the two viewpoints.

Photogrammetrists know that if a scene is photographed from two viewpoints, then the relationship between the camera positions is uniquely determined, in general, by the photographic coordinates of just five distinguishable points; but actually calculating the structure of the scene from five sets of image coordinates involves the iterative solution of five simultaneous third-order equations<sup>5</sup>. I show here that if the scene contains as many as eight points whose images can be located in each projection, then the relative orientation of the two projections, and the structure of the scene, can be computed, in general, from the eight sets of image coordinates by a direct method which

calls for nothing more difficult than the solution of a set of simultaneous linear equations.

Let P be a visible point in the scene, and let  $(X_1, X_2, X_3)$  and  $(X'_1, X'_2, X'_3)$  be its three-dimensional cartesian coordinates with respect to the two viewpoints. The 'forward' coordinates  $X_3$  and  $X'_3$  are necessarily positive. The image coordinates of P in the two views may then be defined as

$$\begin{aligned} (x_1, x_2) &= (X_1/X_3, X_2/X_3), \\ (x'_1, x'_2) &= (X'_1/X'_3, X'_2/X'_3) \end{aligned} \tag{1}$$

and it is convenient to supplement them with the dummy coordinates

$$x_3 = 1, \quad x'_3 = 1 \tag{2}$$

so that one can then write

$$x_\mu = X_\mu/X_3, \quad x'_\nu = X'_\nu/X'_3 \quad (\mu, \nu = 1, 2, 3) \tag{3}$$

As the two sets of three-dimensional coordinates are connected by an arbitrary displacement, we may write

$$X'_\mu = \mathbf{R}_{\mu\nu}(X_\nu - \mathbf{T}_\nu) \tag{4}$$

where  $\mathbf{T}$  is an unknown translational vector and  $\mathbf{R}$  is an unknown rigid rotation matrix. (In this and subsequent equations I sum over repeated Greek subscripts.) The rotation  $\mathbf{R}$  satisfies the relationships

$$\mathbf{R}\bar{\mathbf{R}} = \mathbf{1} = \bar{\mathbf{R}}\mathbf{R}, \quad \det \mathbf{R} = 1 \tag{5}$$

and it is convenient to adopt the length of the vector  $\mathbf{T}$  as the unit of distance:

$$\mathbf{T}^2 (= \mathbf{T}_1^2 + \mathbf{T}_2^2 + \mathbf{T}_3^2) = 1 \tag{6}$$

I begin by establishing a general relationship between the two sets of image coordinates—a relationship which expresses the condition that corresponding rays through the two centres of projection must intersect in space. We define a new matrix  $\mathbf{Q}$  by

$$\mathbf{Q} = \mathbf{R}\mathbf{S} \tag{7}$$

where  $\mathbf{S}$  is the skew-symmetric matrix

$$\mathbf{S} = \begin{bmatrix} 0 & \mathbf{T}_3 & -\mathbf{T}_2 \\ -\mathbf{T}_3 & 0 & \mathbf{T}_1 \\ \mathbf{T}_2 & -\mathbf{T}_1 & 0 \end{bmatrix} \tag{8}$$

Equation (8) may be written as

$$\mathbf{S}_{\lambda\nu} = \epsilon_{\lambda\nu\sigma} \mathbf{T}_\sigma \tag{9}$$

where  $\epsilon_{\lambda\nu\sigma} = 0$  unless  $(\lambda, \nu, \sigma)$  is a permutation of  $(1, 2, 3)$ , in which case  $\epsilon_{\lambda\nu\sigma} = \pm 1$  depending on whether this permutation is even or odd. It follows from equations (4)–(9) that

$$\begin{aligned} X'_\mu \mathbf{Q}_{\mu\nu} X_\nu &= \mathbf{R}_{\mu\kappa} (X_\kappa - \mathbf{T}_\kappa) \mathbf{R}_{\mu\lambda} \epsilon_{\lambda\nu\sigma} \mathbf{T}_\sigma X_\nu \\ &= (X_\lambda - \mathbf{T}_\lambda) \epsilon_{\lambda\nu\sigma} \mathbf{T}_\sigma X_\nu \end{aligned} \tag{10}$$

but because the quantity  $\epsilon_{\lambda\nu\sigma}$  is antisymmetric in every pair of its subscripts, the right-hand side vanishes identically:

$$X'_\mu \mathbf{Q}_{\mu\nu} X_\nu = 0 \tag{11}$$

Dividing equation (11) by  $X_3 X'_3$  we arrive at the desired relationship between the image coordinates:

$$x'_\mu \mathbf{Q}_{\mu\nu} x_\nu = 0 \tag{12}$$

The next step is to determine the nine elements  $\mathbf{Q}_{\mu\nu}$ . There will be one equation of type (12) for every point  $P_i$ , namely

$$(x'_\mu x_\nu)_i \mathbf{Q}_{\mu\nu} = 0 \tag{13}$$

and in this equation the nine quantities  $(x'_\mu x_\nu)_i$  are presumed to be known. The ratios of the nine unknowns  $\mathbf{Q}_{\mu\nu}$  can therefore be obtained, in general, by solving eight simultaneous linear equations of type (13), one for each of eight visible points  $P_1, \dots, P_8$ . I shall not yet discuss the special circumstances under which the solution fails; for the present merely note that if the eight equations (13) are independent, their solution is entirely straightforward from a computational point of view.

The translational vector  $\mathbf{T}$  must be calculated next. Multiplying  $\mathbf{Q}$  on the left of equation (7) by its transpose we obtain

$$\tilde{\mathbf{Q}}\mathbf{Q} = \tilde{\mathbf{S}}\mathbf{R}\mathbf{R}\mathbf{S} = \tilde{\mathbf{S}}\mathbf{S} \quad (14)$$

so that, by the definition of  $\mathbf{S}$ ,

$$\mathbf{Q}_{\mu\nu}\mathbf{Q}_{\mu\sigma} = \mathbf{T}_{\mu}^2\delta_{\nu\sigma} - \mathbf{T}_{\nu}\mathbf{T}_{\sigma} \quad (15)$$

But  $\mathbf{T}_{\mu}^2 = 1$  by equation (6), and so the trace of  $\tilde{\mathbf{Q}}\mathbf{Q}$  must be

$$\mathbf{Q}_{\mu\nu}\mathbf{Q}_{\mu\nu} = \delta_{\nu\nu} - \mathbf{T}_{\nu}^2 = 2 \quad (16)$$

The nine elements of  $\mathbf{Q}$  can therefore be normalized by dividing them by  $\sqrt{2}$  trace  $\tilde{\mathbf{Q}}\mathbf{Q}$ ; the elements of the normalized matrix  $\tilde{\mathbf{Q}}\mathbf{Q}$  can then be used for computing the ratios of the components of  $\mathbf{T}$ :

$$\tilde{\mathbf{Q}}\mathbf{Q} = \begin{bmatrix} 1 - \mathbf{T}_1^2 & -\mathbf{T}_1\mathbf{T}_2 & -\mathbf{T}_1\mathbf{T}_3 \\ -\mathbf{T}_2\mathbf{T}_1 & 1 - \mathbf{T}_2^2 & -\mathbf{T}_2\mathbf{T}_3 \\ -\mathbf{T}_3\mathbf{T}_1 & -\mathbf{T}_3\mathbf{T}_2 & 1 - \mathbf{T}_3^2 \end{bmatrix} \quad (17)$$

There are evidently three independent relationships between the diagonal and the off-diagonal elements of  $\tilde{\mathbf{Q}}\mathbf{Q}$ ; these supply three independent checks on the results obtained so far. The absolute signs of the  $\mathbf{T}_{\mu}$  and the  $\mathbf{Q}_{\mu\nu}$  are still undetermined but, as we shall see, these ambiguities are easily resolved later.

We are now in a position to compute the elements of the rotation matrix  $\mathbf{R}$ . First note that equation (7) has a simple interpretation in terms of vector products. If we regard each row of  $\mathbf{Q}$ , and each row of  $\mathbf{R}$ , as a vector, then

$$\mathbf{Q}_{\alpha} = \mathbf{T} \times \mathbf{R}_{\alpha} \quad (\alpha = 1, 2, 3) \quad (18)$$

and the condition for  $\mathbf{R}$  to represent a proper rotation can be expressed in a similar form:

$$\mathbf{R}_{\alpha} = \mathbf{R}_{\beta} \times \mathbf{R}_{\gamma} \quad (19)$$

for  $\alpha, \beta, \gamma$  such that  $\epsilon_{\alpha\beta\gamma} = 1$ . The problem is then to express the  $\mathbf{R}_{\alpha}$  in terms of  $\mathbf{T}$  and the  $\mathbf{Q}_{\alpha}$ .

By equation (18),  $\mathbf{R}_{\alpha}$  is orthogonal to  $\mathbf{Q}_{\alpha}$  and may therefore be expressed as a linear combination of  $\mathbf{T}$  and  $\mathbf{Q}_{\alpha} \times \mathbf{T}$ . We therefore introduce new vectors

$$\mathbf{W}_{\alpha} = \mathbf{Q}_{\alpha} \times \mathbf{T} \quad (\alpha = 1, 2, 3) \quad (20)$$

and write

$$\mathbf{R}_{\alpha} = a_{\alpha}\mathbf{T} + b_{\alpha}\mathbf{W}_{\alpha} \quad (21)$$

Substitution into equation (18) gives

$$\mathbf{Q}_{\alpha} = \mathbf{T} \times (a_{\alpha}\mathbf{T} + b_{\alpha}\mathbf{W}_{\alpha}) = b_{\alpha}(\mathbf{T} \times \mathbf{W}_{\alpha}) \quad (22)$$

But as  $\mathbf{T}$  is a unit vector,

$$\mathbf{T} \times \mathbf{W}_{\alpha} = \mathbf{T} \times (\mathbf{Q}_{\alpha} \times \mathbf{T}) = \mathbf{Q}_{\alpha} \quad (23)$$

and so

$$b_{\alpha} = 1 \quad (24)$$

Turning to equation (19) we deduce that when  $\epsilon_{\alpha\beta\gamma} = 1$ ,

$$\begin{aligned} a_{\alpha}\mathbf{T} + \mathbf{W}_{\alpha} &= (a_{\beta}\mathbf{T} + \mathbf{W}_{\beta}) \times (a_{\gamma}\mathbf{T} + \mathbf{W}_{\gamma}) \\ &= a_{\beta}\mathbf{Q}_{\gamma} - a_{\gamma}\mathbf{Q}_{\beta} + \mathbf{W}_{\beta} \times \mathbf{W}_{\gamma} \end{aligned} \quad (25)$$

But in equation (25) the vectors  $\mathbf{W}_{\alpha}$ ,  $\mathbf{Q}_{\beta}$  and  $\mathbf{Q}_{\gamma}$  are all orthogonal to  $\mathbf{T}$ , whereas  $\mathbf{W}_{\beta} \times \mathbf{W}_{\gamma}$  is, by equation (20), a multiple of  $\mathbf{T}$ . It follows that in equation (25) the first term on the left equals the last term on the right,

$$a_{\alpha}\mathbf{T} = \mathbf{W}_{\beta} \times \mathbf{W}_{\gamma} \quad (26)$$

and equation (21) finally becomes

$$\mathbf{R}_{\alpha} = \mathbf{W}_{\alpha} + \mathbf{W}_{\beta} \times \mathbf{W}_{\gamma} \quad (27)$$

Having obtained in this way the vector  $\mathbf{T}$  and the three rows of the matrix  $\mathbf{R}$ , we can at last find the three-dimensional coordinates  $X_{\mu}$ , as follows:

By equation (4),

$$X'_{\mu} = \mathbf{R}_{\mu\nu}(X_{\nu} - \mathbf{T}_{\nu})$$

from which it follows that

$$x'_1 = \frac{X'_1}{X'_3} = \frac{\mathbf{R}_{1\nu}(X_{\nu} - \mathbf{T}_{\nu})}{\mathbf{R}_{3\nu}(X_{\nu} - \mathbf{T}_{\nu})} \quad (28)$$

Introducing the vectors

$$\mathbf{X} = (X_1, X_2, X_3), \quad \mathbf{x} = (x_1, x_2, 1) \quad (29)$$

we may write equation (28) in terms of the rows  $\mathbf{R}_{\alpha}$  of the matrix  $\mathbf{R}$ :

$$x'_1 = \frac{\mathbf{R}_1 \cdot (\mathbf{X} - \mathbf{T})}{\mathbf{R}_3 \cdot (\mathbf{X} - \mathbf{T})} = \frac{\mathbf{R}_1 \cdot (\mathbf{x} - \mathbf{T}/X_3)}{\mathbf{R}_3 \cdot (\mathbf{x} - \mathbf{T}/X_3)} \quad (30)$$

from which it follows that

$$X_3 = \frac{(\mathbf{R}_1 - x'_1\mathbf{R}_3) \cdot \mathbf{T}}{(\mathbf{R}_1 - x'_1\mathbf{R}_3) \cdot \mathbf{x}} \quad (31)$$

The other unprimed coordinates are then given by equation (3) as

$$X_1 = x_1 X_3, \quad X_2 = x_2 X_3 \quad (32)$$

and the primed coordinates are finally obtained from equation (4).

There are, in fact, four distinct solutions to the problem, associated with the alternative choices of sign for the components of  $\mathbf{T}$  and the elements of  $\mathbf{Q}$ . But any doubt as to which choices to adopt is easily resolved: the condition that the forward coordinates of any point must both be positive will be satisfied if, and only if, both sets of signs are correctly chosen.

There are certain 'degenerate' eight-point configurations for which the algorithm fails because the associated equations (13) become non-independent. A configuration will be degenerate if as many as four of the points lie in a straight line, or if as many as seven of them lie in a plane. Quite unexpectedly, degeneracy also arises if the configuration includes six points at the vertices of a regular hexagon, or consists of eight points at the vertices of a cube. The 'invisibility' of such configurations to the eight-point algorithm may be demonstrated by arguments too long to be presented here; but the reasons for it are unconnected with any ambiguity in the interpretation of the resulting projections. A degenerate configuration immediately becomes 'visible', however, if one of the offending points  $P_i$  is moved slightly away from its original position.

In general, then, the three-dimensional coordinates of a set of eight or more visible points may be obtained by the following algorithm:

- (1) Set up eight equations of the form (13), and solve them for the ratios of the nine unknowns  $\mathbf{Q}_{\mu\nu}$ .
- (2) Compute the matrix  $\tilde{\mathbf{Q}}\mathbf{Q}$  and normalize the elements of  $\mathbf{Q}$  by dividing them by  $\sqrt{2}$  trace  $\tilde{\mathbf{Q}}\mathbf{Q}$ .
- (3) Obtain the magnitudes and the relative signs of the  $\mathbf{T}_{\nu}$  from equation (17); their absolute signs, and those of the  $\mathbf{Q}_{\mu\nu}$ , may have to be chosen arbitrarily at this stage.
- (4) Define three new vectors by equation (20) and use equation (27) to calculate the rows of the matrix  $\mathbf{R}$ .
- (5) Use equations (31) and (32) for computing the unprimed three-dimensional coordinates of all the visible points, and equation (4) for calculating the primed coordinates.
- (6) Check that the forward coordinates  $X_3$  and  $X'_3$  of any point are both positive. If both signs are negative, alter the signs of the  $\mathbf{T}_{\nu}$  and return to step (5); if  $X_3$  and  $X'_3$  are of opposite sign, reverse the signs of the  $\mathbf{Q}_{\mu\nu}$  and return to step 4.

The algorithm yields the most accurate results when applied to situations in which the distance  $D$  between the centres of projection is not too small compared with their distances from the points  $P_i$ . If the projective coordinates are accurate to a few seconds of arc, the forward coordinates of the  $P_i$  can be estimated out to about  $10D$  with great accuracy, and even as far as  $100D$  if the  $P_i$  are adequately spaced in depth. This performance is comparable with that of the human visual system; but that does not, of course, imply that the eight-point algorithm is actually used in stereoscopic vision, as in binocular vision we

have at least some information about the relative orientation of the two eyes. The most useful applications of the eight-point algorithm will probably be found in computer vision systems, where there is still a need for fast and accurate methods of converting two-dimensional images into three-dimensional interpretations.

I thank Drs A. L. Allan and K. B. Atkinson for the reference to Thompson<sup>1</sup>, and the RS and SRC for support.

Received 13 April; accepted 13 July 1981.

1. Thompson, E. H. *Photogrammetric Record* 3(14), 152-159 (1959).
2. Ogle, K. N. *Researches in Binocular Vision* (Hafner, New York, 1964).
3. Ullman, S. *The Interpretation of Visual Motion* (MIT Press, Cambridge, 1979).
4. Marr, D. & Poggio, T. *Science* 194, 283-287 (1976).

## Local extinction and ecological re-entry of early Eocene mammals

David M. Schankler

Department of Geological and Geophysical Sciences, Princeton University, Princeton, New Jersey, USA

The use of high-resolution stratigraphical control in studying the species sequencing patterns of early Eocene mammals has recently been demonstrated by Gingerich *et al.*<sup>1-5</sup>. These studies have documented the nature of the tempo and mode of evolution and have stimulated the debate between adherents of phyletic gradualism and punctuated equilibria<sup>6</sup>. All studies have been largely verticalist (evolutionary) in outlook, equating change within a single basin of deposition with evolution. However, when I applied these techniques to the early Eocene condylarth, *Phenacodus*, I found a strong lateral (biogeographical and ecological) component influencing the sequencing of species in a single basin. I report here that *Phenacodus* species are relatively static in size and morphology throughout the local section studied, and two of these show statistically significant discontinuities in temporal range. The clumped re-entry of these species after local disappearance along with the introduction of other new taxa points to ecological control of vertical events within a local section.

I used high-resolution stratigraphy to study mammalian evolution at the species level, concentrating on early Eocene Willwood Formation of northwestern Wyoming because of the density and continuity of the fossil record preserved in these sediments. The Elk Creek Section through the Willwood

Formation of the central Bighorn Basin is 773 m thick<sup>7</sup>, and represents an estimated 3.5 Myr (ref. 8). Using a 10-m resolution interval, over 240 fossil localities can be related to this section. These localities, distributed over a 650-km<sup>2</sup> area, so far have produced over 15,000 specimens and are distributed vertically through the section so that more than 50 of the 77 10-m intervals are fossiliferous; half of these have total mammalian sample sizes (minimum number of individuals) of over 75.

In a recent review of the systematics of the genus *Phenacodus*, West<sup>9</sup> recognized three species from the early Eocene, *P. brachypternus*, *P. vortmani* and *P. primaevus*; his study predates publication of the Elk Creek Section and the stratigraphical resolution used was at the level of the zone, that is, early Eocene *Phenacodus* were divided into three samples corresponding to Graybullian (base-530 m), Lysitian (530-660 m) and Lostcabinian (660-770 m) zones. *P. brachypternus* was recorded as being almost wholly restricted to the Graybullian, whereas the other two species were distributed through the entire Wasatchian. *P. brachypternus* and *P. vortmani* are relatively well defined fossil species that have always been easily identified in collections on the basis of size and morphology, whereas *P. primaevus* has usually been characterized by a fairly large variation that has made it difficult to define the bounds of the species. This has led to the subdivision of *P. primaevus* into two to four species<sup>10,11</sup>. West<sup>9</sup> did not subdivide this species even though the recorded ranges of variation (coefficients of variation of ~10 for most linear measures) and a range of ln 0.8 for tooth crown area of M<sub>2</sub> (lower second molar) are almost double those expected for a single species<sup>12-14</sup>.

Inclusion of all large specimens of *Phenacodus* in a single species is untenable, and on the basis of data shown in Fig. 1, the large phenacodontids have been subdivided into two species, *P. intermedius* and *P. primaevus*. As previously shown by Gingerich<sup>12,13</sup> and observed in the two smaller species of *Phenacodus*, the normal range of variation of ln of the crown area of a molar tooth is of the order of 0.4. In the interval 100-190 m, almost all specimens fall neatly within the expected range of a single species, the size of which agrees well with the type of *P. intermedius*; thus these specimens are referred to that species. The single outlier at the 100-m level has a value that differs by 4 standard deviations from the mean of *P. intermedius* specimens, and is therefore too large to be included in that species. In the interval 200-380 m there is a second well defined

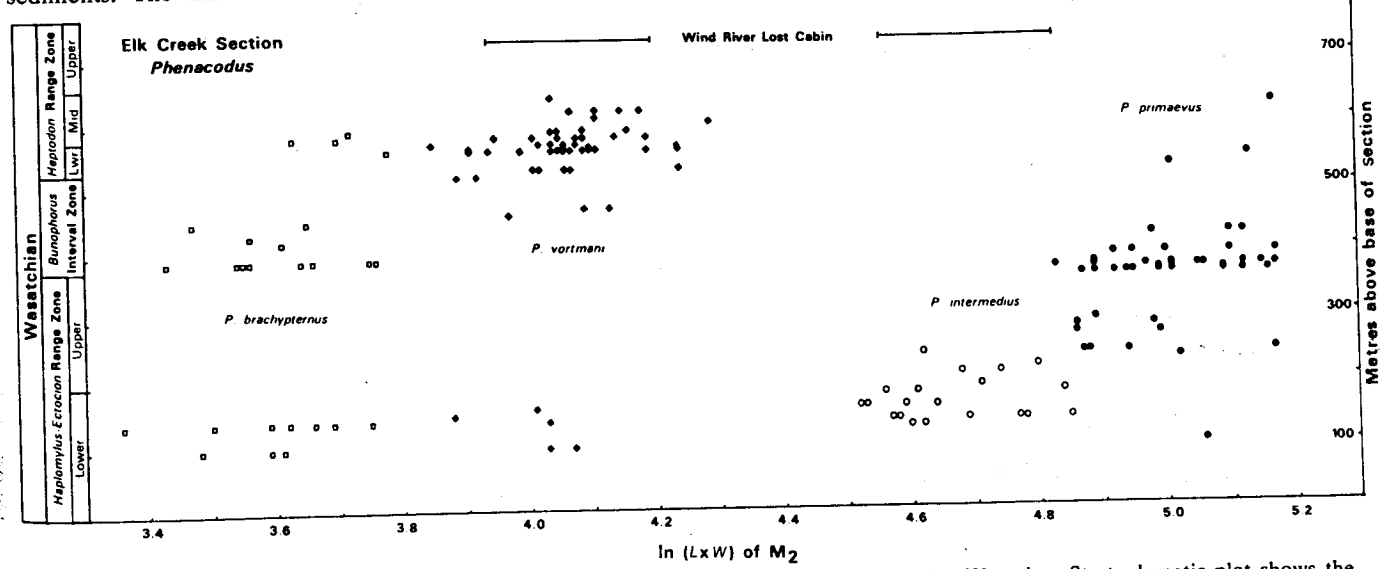


Fig. 1 Species-sequencing pattern of early Eocene *Phenacodus* in the central Bighorn Basin, Wyoming. Stratophenetic plot shows the distribution in size and time of the four species, and illustrates the discontinuity in the temporal ranges of *P. brachypternus* (□) and *P. vortmani* (◆), and the transition in dominance between *P. intermedius* (○) and *P. primaevus* (●) at the base of the Upper Haplomyilus-Eocene Zone. Size is measured on the abscissa as ln of the crown area of the lower second molar (M<sub>2</sub>) and time is shown on the ordinate as metres above the base of the Elk Creek Section. The horizontal lines at the 730-m level are the maximum ranges of the two species of *Phenacodus* from the Lostcabinian of the Wind River Basin. Note the similarity between the size range of the larger species from the Wind River Basin and *P. intermedius* from the Elk Creek Section.